Mon. Not. R. Astron. Soc. **000**, 000–000 (0000) Printed 21 February 2014 (MN LATEX style file v2.2)

Dust Formation By Failed Supernovae

C. S. Kochanek[1,2]
[1] *Department of Astronomy, The Ohio State University, 140 West 18th Avenue, Columbus OH 43210*
[2] *Center for Cosmology and AstroParticle Physics, The Ohio State University, 191 W. Woodruff Avenue, Columbus OH 43210*

arXiv:1402.4812v1 [astro-ph.SR] 19 Feb 2014

21 February 2014

ABSTRACT
We consider dust formation during the ejection of the hydrogen envelope of a red supergiant during a failed supernova (SN) creating a black hole. While the dense, slow moving ejecta are very efficient at forming dust, only the very last phases of the predicted visual transient will be obscured. The net grain production consists of $M_d \sim 10^{-2} M_\odot$ of very large grains (10 to 1000μm). This means that failed SNe could be the source of the very large extrasolar dust grains identified by *Ulysses*, *Galileo* and radar studies of meteoroid re-entry trails rather than their coming from an ejection process associated with protoplanetary or other disks.

Key words: stars: supernovae:general: dust: black holes

1 INTRODUCTION

The formation of black holes during a failed supernova (SN) has generally been assumed to lead to a black hole with the mass of the star at the time core collapse is initiated (e.g. Heger et al. 2003). Nadezhin (1980) argued that this was not true of red supergiants because the hydrogen envelope is so weakly bound that the drop in the gravitational potential created by neutrino losses is enough to unbind the envelope. Radiation hydrodynamic simulations by Lovegrove & Woosley (2013) confirmed this supposition. Failed SNe of red supergiants lead to the formation of black holes with (roughly) the mass of the helium core of the star at the time of collapse and not the total mass of the star.

This new expectation is of particular interest because studies of SN progenitors appear to be finding too few massive progenitors (Kochanek et al. 2008) particularly in the upper end of the red supergiant mass range (Smartt et al. 2009). Smartt et al. (2009) estimated that red supergiant progenitors were missing from $(16.5 \pm 1.5) M_\odot$ to the upper mass limit for stars to explode as red supergiants and become Type IIP SNe (25-30$M_\odot$). This is an interesting mass range for failed SNe because theoretical studies indicate that many stellar models in this mass range have density structures that make it more difficult to produce a successful explosion (e.g. O'Connor & Ott 2011, Ugliano et al. 2012). Other options include changing stellar models so that stars in this mass range do not end their lives as red supergiants (e.g. Groh et al. 2013) or using dusty winds to make them less observable (e.g. Walmswell & Eldridge 2012, but see Kochanek et al. 2012).

Producing failed SNe in this mass range also provides a natural explanation for the observed distribution of remnant masses (Kochanek 2013). The remnant mass function is bimodal between neutron stars with masses near $1.4 M_\odot$ and black holes with masses of 5-10$M_\odot$, although it is uncertain if the gap in the mass function is truly empty or simply a deep minimum (e.g. Bailyn et al. 1998, Özel et al. 2010, Farr et al. 2011, Kreidberg et al. 2012). This gap is difficult to explain if black holes form by fall back of material in a successful explosion (e.g. Zhang et al. 2008, Fryer et al. 2012). The gap is, however, a natural consequence of combining supernovae without fall back, which best explain the masses observed in neutron star binaries (Pejcha et al. 2012), with a population of $\sim 20 M_\odot$ failed supernovae where the typical black hole mass of $\sim 7 M_\odot$ is simply the typical helium core mass of the failed SNe.

Lovegrove & Woosley (2013) also pointed out that the ejection of the envelope would be associated with a relatively long lived ($\sim$ year), modest luminosity ($\sim 10^6 L_\odot$) transient largely powered by the recombination of the envelope. We have been carrying out a search for failed SNe using the Large Binocular Telescope following the ideas of Kochanek et al. (2008), where we monitor nearby galaxies to see if any stars effectively vanish, potentially with some intervening transient phenomenon. This survey can easily identify the transients predicted by Lovegrove & Woosley (2013), although it is not well suited for identifying the shorter ($\sim$ week) shock break out peak associated with the event (see Piro 2013).

These more massive red supergiants tend to have winds that produce silicate dusts and other products of oxygen-rich chemistry (see, e.g., the review by Cherchneff 2013), and, as mentioned earlier, Walmswell & Eldridge (2012) even propose using this obscuration as a possible means of solving the red supergiant problem identified by Smartt et al. (2009). During the envelope ejection following a failed SNe, this same material is going to be ejected *en masse* at much

higher densities and only moderately higher velocities, so presumably it is also likely to form dust but in much greater quantities. This leads to the possibility that the optical properties of the transient are greatly modified from the dust free simulations carried out by Lovegrove & Woosley (2013).

We already know of one class of transients that successfully cloaks themselves in dust following their peaks, the SN 2008S class of explosive transients from AGB stars (see, e.g., Thompson et al. 2009, Kochanek 2011a, Szczygieł et al. 2012). The mechanism here is very different, since the dust in the SN 2008S class is almost certainly dust re-forming in a pre-existing dense wind after being destroyed by the transient (Kochanek 2011a). However, it does suggest an investigation of whether the visual transient predicted by Lovegrove & Woosley (2013) will be substantially modified by dust formation and if the ejected dust has any consequences for our understanding of the interstellar medium. In §2 we model dust formation in these systems to find that the transients are not substantially modified even though they should be very efficient at forming significant masses of very large dust grains. We discuss the implications in §3.

2 DUST FORMATION

A striking property of these transients is the ejection of the hydrogen envelope under conditions that seem remarkably conducive to the formation and growth of dust grains. The densities are very high compared to stellar winds that easily form dust and the transient luminosities and temperatures are relatively low. Following our previous examination of dust formation in Luminous Blue Variable (LBV) eruptions (Kochanek 2011b), we adopt the physically reasonable view that particle nucleation simply occurs once conditions allow nucleation, and that we must then follow the collisional growth of the grains to estimate the resulting opacities and optical depths. From Lovegrove & Woosley (2013) we have the transient temperature and luminosity, $T_*(t)$ and $L_*(t)$, and the density and velocity profile at some late time t_0 for their $15M_\odot$ models with ejecta kinetic energies of 3.8 and 8.9×10^{47} ergs. At these late phases, we can view the ejecta as being in free expansion, so the velocity $v_p(r_p)$ is now time independent. Hence, the radius of the material at some other time t is simply $r(t) = r_p + (t-t_p)v_p(r_p)$ and at late times the density $\rho(t)$ is related to the mass of the zone by $m = 4\pi v_p^2 \Delta v_p t^3 \rho(t) = 4\pi(\Delta v_p/v_p) r_p(t)^3 \rho(t)$ where m is the mass in the zone and Δv_p is the velocity difference across the zone edges.

Since the radiation from these transients is cold ($T_* \sim$ 3000-4000 K, Lovegrove & Woosley 2013), there is no ultraviolet radiation that can stochastically heat dust grains as they try to form (this is the mechanism that prevents dust formation around hot stars, see Kochanek 2011b). We need only consider whether the equilibrium temperature of a small grain is lower than the temperature at which grains can form. This leads to the requirement that dust can only form once the ejecta is more distant than the time-dependent dust formation radius

$$R_f(t) = \left(\frac{L_*(t) Q_P(T_*(t))}{16\pi Q_P(T_f)\sigma T_f^4}\right)^{1/2} \tag{1}$$

where $Q_P(T)$ is the Planck mean absorption factor and $T_f \sim$ 1000 to 2000 K is the dust formation temperature. We use the values for the smallest grain sizes ($a = 10^{-3}\mu$m) given by Draine & Lee (1984) and Laor & Draine (1993). Figure 1 compares the evolution of $R_f(t)$ to the photosphere defined by $R_{phot}(t) = (L_*(t)/4\pi\sigma T_*(t)^4)^{1/2}$ and to the radius of the outermost ejecta. We find that the ejecta are inside the $R_f(t)$ until very late in the transient, so the first key result is that dust formation can only affect the late phases of the transient.

Note that if the gas is cooling adiabatically, the gas temperature is essentially guaranteed to be lower than the dust formation temperature at the time dust formation commences. We can normalize the gas temperature such that it has the photospheric temperature when it is at the photosphere, so $T_{gas}(R) = T_*(R_{phot}/R)^2$ (for $\gamma = 5/3$). When the gas temperature reaches the formation temperature, $T_{gas} = T_f$, then the dust temperature (ignoring Planck factors) due to the radiation field of $T_d = T_f(T_*/T_f)^{3/4} > T_f$ will always exceed the dust formation temperature unless there is a precipitate drop in the luminosity. We explicitly checked this point as part of the calculation including the time variability of the luminosity and found that dust formation was always limited by radiative heating rather than adiabatic cooling.

We simply assume that nucleation occurs, and then allow the dust to grow collisionally. The grain radius grows as

$$\frac{da}{dt} = \frac{v_c X_d \rho}{4\rho_{bulk}} \tag{2}$$

where v_c is the typical collisional velocity, X_d is the mass fraction of the species condensing onto the grains, ρ is the gas density, and $\rho_{bulk} \simeq 2.2$ or 3.8 g cm^{-3} is the bulk density of the graphitic or silicate grains (e.g. Kwok 1975, Deguchi 1980). If we normalize the density to the value at the formation radius $\rho = \rho_f(t_f/t)^3$ and scale the collision velocities as $v_c = v_{cf}(t_f/t)^n$, then we can integrate Equation 2 to get the final size of the grains

$$a_f = \frac{v_{cf} R_f X \rho_f}{4(n+2) v \rho_{bulk}}. \tag{3}$$

The size at any intermediate time is simply

$$a(t) = a_f\left[1 - \left(\frac{R_f(t_f)}{r(t)}\right)^{n+2}\right] \tag{4}$$

where $t > t_f$ and t_f is the time the fluid element started to form dust. Because growth is a collisional process, the rapidly dropping density means that most of the growth occurs between R_f and $2R_f$. As a result, the choice for the velocity scaling exponent n is unimportant given the other uncertainties and we will simply use $n = 0$. Here we have used a sticking probability of unity and ignored coagulation, where the former slows and the latter speeds growth. We will scale the amount of condensible material to $X = 10^{-3}X_3$, since silicate dust formation is more likely than carbonaceous dust given the properties of the winds of these stars. Given the temperatures near the dust formation radius, we adopt $v_c = 1$ km/s as a reasonable collision velocity. Changing these values allows moderate changes in the grain sizes but leads to no qualitative changes.

As a check, we can apply this approach to a wind with mass loss rate $\dot{M} = 10^{-5}\dot{M}_5 M_\odot$ year^{-1} and velocity $v_w =$

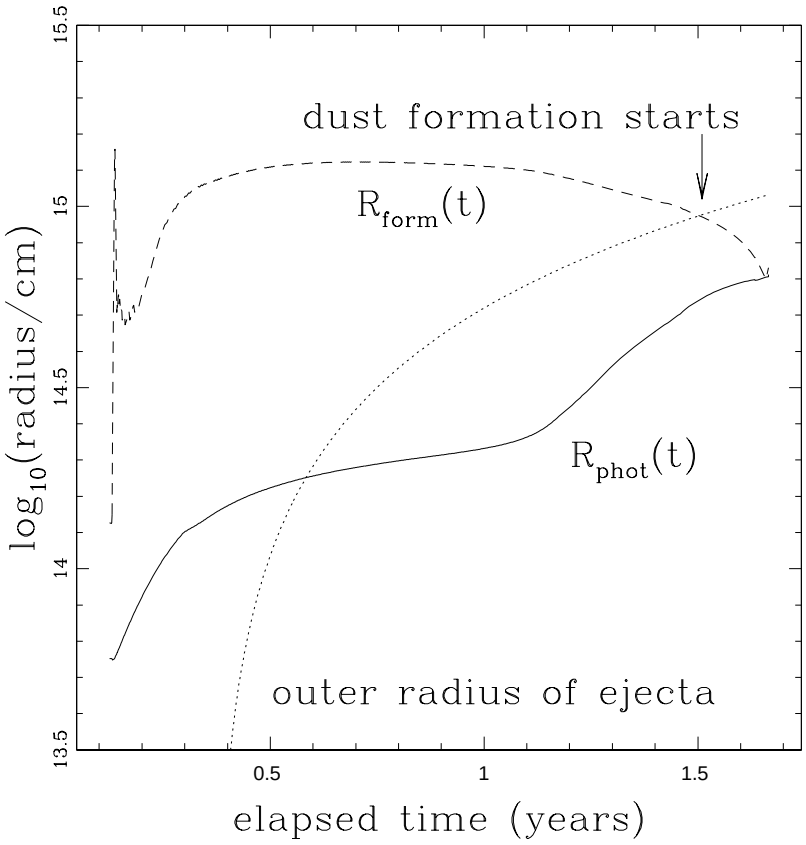

Figure 1. Evolution of the photospheric radius $R_{phot}(t)$ (solid), the outer radius of the ejecta (dotted) and the dust formation radius $R_f(t)$ (dashed) for the lower energy transient. Dust formation starts after 1.5 years when the outer radius of the ejecta becomes larger than R_f, as indicated by the arrow. Here we used $T_f = 1200$ K and silicate dust. The outer radius simply uses the final velocity without the accelerations that would make it converge with R_{phot} at early times.

$10v_{w10}$ km/s around a star with luminosity $L_* = 10^4 L_{*4} L_\odot$. A silicate grain has an equilibrium temperature $T_f = 1200$ K at $R_f \simeq R_{f14} 10^{14}$ cm, implying a final grain size of

$$a_f = \frac{\alpha v_c X \dot{M}}{16\pi\rho_b v_w^2 R_f} \simeq 0.01 \frac{\alpha \dot{M}_5 X_3 v_{c1}}{R_{f14} v_{w10}^2} \mu\mathrm{m} \quad (5)$$

for a constant velocity wind with $\rho = \dot{M}/4\pi v_w r^2$. This is the correct order of magnitude for dust formation around an asymptotic giant branch (AGB) star with these properties. For example, Nanni et al. (2013) find $a_f \simeq 0.1\mu$m for $X_3 \simeq 3$, while our simple expression would give $a_f \simeq 0.03\mu$m. The estimate is low because the constant velocity assumption underestimates the time spent near R_f as the formation of dust accelerates the flow. For dust formation in the ejecta of a transient, this issue does not arise because the velocities are not controlled by the dust formation process.

Figure 2 shows the final grain sizes for silicate dust formed by failed SNe assuming $T_f = 1200$ K. Graphitic grains are larger roughly by the ratio of the bulk densities. The smaller scale structures in Figure 2 are caused by fluctuations in the velocity divergence Δv of the individual Lagrangian zones in the velocity profile from Lovegrove & Woosley (2013) that would average out over the expansion time but are present in an instantaneous snap shot of the ejecta. As expected, these transients offer excellent conditions for the growth of grains, with peak sizes for our nominal parameters on the scale of millimeters. With $M_{tot} = 8M_\odot$ of ejecta, the net dust production is $M_{dust} = XM_{tot} \sim 10^{-2} M_\odot$ of dust. There is some freedom to adjust the final sizes by changing the parameters (X, v_{cf}, n) in Equation 3, but not enough freedom to change the qualitative result that failed SNe should produce a significant mass of very large dust grains.

At any given time, we can now determine which of the Lagrangian zones from the Lovegrove & Woosley (2013) simulations have passed their dust formation radius, and the size to which the grains have grown since that time. We then calculate the visual (V-band) opacities of these layers using the scaled cross sections $Q_V(a)$. The optical depth is then

$$\tau(t) = \int dr \frac{3X\rho(r,t)Q(a(r,t))}{4\rho_{bulk} a(r,t)} \quad (6)$$

where the integral extends from the dust formation radius $R_f(t)$ from Equation 1 to the outer edge of the star, and the density $\rho(r,t)$ and grain size $a(r,t)$ are functions of both radius and time. We separately calculate the absorption τ_{abs} and scattering τ_{sca} optical depths, again using Draine & Lee (1984) and Laor & Draine (1993) for the values of Q_V, and then use the approximation that the effective total absorption optical depth is $\tau_{eff} = (\tau_{abs}(\tau_{abs} + \tau_{sca}))^{1/2}$.

In practice, as soon as dust formation is permitted, the transient is blacked out, as shown in Figure 3. This is sim-

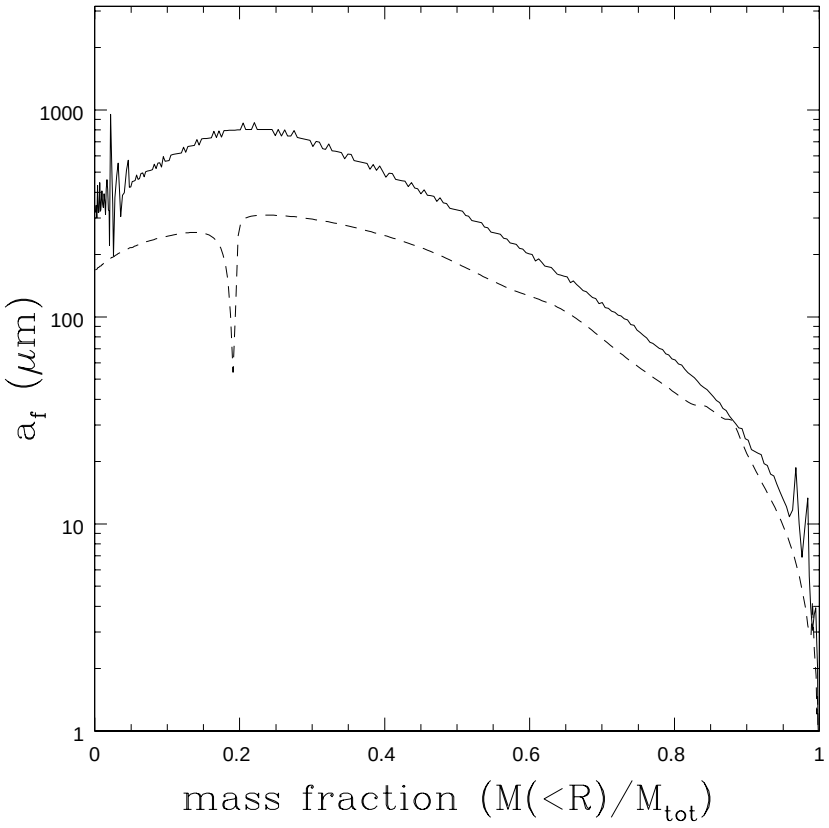

Figure 2. Final silicate grain sizes a_f as a function of the ejecta mass fraction $M(< R)/M_{tot}$ for the low (solid) and high (dashed) energy transients. The fine structures in the curves are due to structures in the velocity difference Δv across the Lagrangian zones of the Lovegrove & Woosley (2013) simulations. Here we used $T_f = 1200$ K.

ply a consequence of the relatively small R_f and the enormous amount of mass – in the first 10 days of this period, $0.1M_\odot$ of material moves beyond the formation radius of order $R_f \simeq 5 \times 10^{15}$ cm. This material will have an optical depth of $\tau \simeq 2.5\kappa$, where κ is the opacity. Typical dusty materials have $\kappa_V \sim 10^2$, which means that the optical depth will be large even if dust formation is very inefficient. As the source vanishes in the optical, it would be replaced by a near/mid-IR source with an initial temperature near the dust formation temperature. It would rapidly become colder and fainter due to the combined effects of the collapsing luminosity and the increasing optical depth. This phase might be observable for a brief period (weeks) with JWST.

3 DISCUSSION

Despite having very favorable conditions for dust formation, the optical signature of a failed SNe from a red supergiant will be little affected by dust formation. Failed SNe are, however, very efficient at producing dust compared to successful SNe. Keeping all else fixed, the final grain size in Equation 3 is $a_f \propto (vL_*)^{-1}$ because the growth rate at the dust formation radius scales as $da/dt \propto R_f^{-3} \propto L_*^{-3/2}$ while the time scale over which the growth occurs is $R_f/v \simeq L_*^{1/2}/v$. Since for a failed SNe $v \simeq 10^2$ km/s and $L_* \simeq 10^6 L_\odot$ and for a successful SNe $v \simeq 5000$ km/s and $L_* \simeq 10^9 L_\odot$, the nominal final size ratio of $a_{fail}/a_{succ} \sim 50000$ gives a sense of the difference. The hotter radiation temperature of successful SNe further favors the failed SNe. The one advantage for the successful SNe is that the heavily metal enriched material outside the iron core is also ejected, so some fraction of the ejecta from a SNe has a condensible fraction of $X \sim 10^{-1}$ instead of $X \sim 10^{-3}$ for the envelope of a red supergiant. Somewhat surprisingly, even the very metal rich ejecta of real SNe have slower dust growth rates than the envelope of a failed SN.

The conditions are so favorable for dust formation that the grains formed in this scenario are enormous – up to $a_f \sim 1$ mm in size. This is interesting because several recent experiments have found evidence for a significant population of very large extrasolar dust grains. Impact detectors on the *Ulysses* and *Galileo* spacecraft (Landgraf et al. 2000, Krüger et al. 2007) measured a significant flux of large grains entering the heliosphere up to their detection limit of $a \simeq 1\mu$m, and still larger 10-30μm grains of apparently extrasolar origin have been found by ground-based radar studies of meteoroid re-entry trails (e.g. Meisel et al. 2002, Baggaley 2000). The resulting rates appear to be consistent with simply extending the roughly logarithmic distribution of grain masses, $m(dn/dm) \propto m^{-1.1}$, (e.g. Murray et al. 2004, Draine 2009) well beyond the standard truncation scale of the models for dust in the interstellar medium (ISM) at $a \sim 0.1\mu$m.

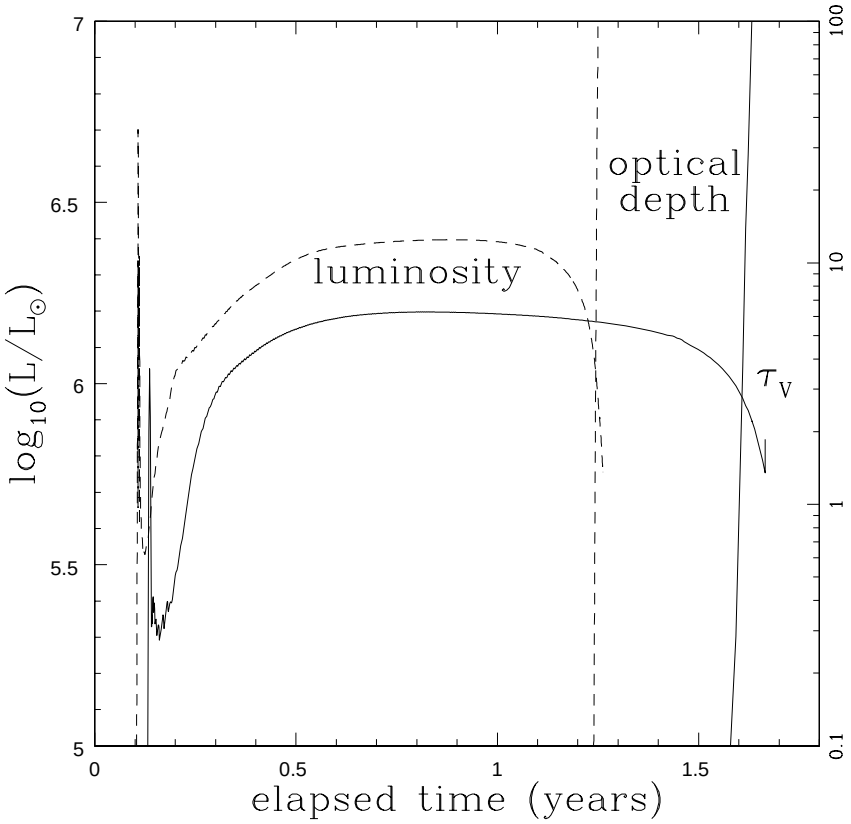

Figure 3. The transient luminosity from Lovegrove & Woosley (2013) (right scale) and the dust visual optical depth τ_V (right scale) for the low (solid) and high (dashed) energy transients. As soon as dust formation becomes feasible, the optical depth becomes "infinite" and will black out the already rapidly fading transient. The initial luminosity spike occurs when the low velocity shock wave causing the ejection first reaches the stellar surface (see Piro 2013). Here we used $T_f = 1200$ K and silicate dust

There has been no natural source of these very large grains because even the most extreme stellar winds have natural size cutoffs of order 1μm. There there are grains with AGB star compositions as large as 10μm found in meteorites, but they are rare (Zinner 1998). For still larger grains, ejection from proto-planetary disks may be possible (see Murray et al. 2004). These failed SNe would produce $\sim 10\%$ of all dust mass (assuming SN and stars produce comparable amounts of dust) with a mechanism that both naturally creates and ejects the grains into the interstellar medium (ISM) at relatively low velocities so as to minimize sputtering.

Quantitatively, this would be too little mass to explain the solar system results. However, there is almost certainly a problem with the solar system abundance normalizations because simply extending the ISM size distribution (e.g. Draine 2003) to larger sizes would lead to an abnormal average extinction curve ($R_V \simeq 5.8$) and require a greater abundance of condensible species (C, O, Fe, etc.) than is available (Draine 2009). Possible solutions include a local anomaly in the grain size distribution (Draine 2009), propagation effects from the ISM into the solar system (Slavin et al. 2012) or that the source of the grains is not actually extrasolar (Belyaev & Rafikov 2010). The small dust mass fraction from failed SNe would not create these problems. Socrates & Draine (2009) discuss a means of directly detecting large grains in the ISM as a scattered light halo during optical transients. At present, however, it seems that interest in these large grains has waned – a relation to black hole formation, however bizarre, might provide a motivation to resolve these issues.

ACKNOWLEDGMENTS

I am grateful to E. Lovegrove and S. Woosley for sharing the results of their simulations so that these calculations could be performed, to N. Murray for discussions of large dust grains, and to T.A. Thompson for comments and discussions.

REFERENCES

Baggaley, W. J. 2000, Journal of Geophysical Research, 105, 10353
Bailyn, C. D., Jain, R. K., Coppi, P., & Orosz, J. A. 1998, ApJ, 499, 367
Belyaev, M. A., & Rafikov, R. R. 2010, ApJ, 723, 1718
Cherchneff, I. 2013, EAS Publications Series, 60, 175
Deguchi, S. 1980, ApJ, 236, 567
Draine, B. T., & Lee, H. M. 1984, ApJ, 285, 89

Draine, B. T. 2003, ARA&A, 41, 241
Draine, B. T. 2009, Space Science Reviews, 143, 333
Farr, W. M., Sravan, N., Cantrell, A., et al. 2011, ApJ, 741, 103
Fryer, C. L., Belczynski, K., Wiktorowicz, G., et al. 2012, ApJ, 749, 91
Groh, J. H., Meynet, G., Georgy, C., & Ekström, S. 2013, A&A, 558, A131
Heger, A., Fryer, C. L., Woosley, S. E., Langer, N., & Hartmann, D. H. 2003, ApJ, 591, 288
Kochanek, C. S., Beacom, J. F., Kistler, M. D., et al. 2008, ApJ, 684, 1336
Kochanek, C. S. 2011a, ApJ, 741, 37
Kochanek, C. S. 2011b, ApJ, 743, 73
Kochanek, C. S., Khan, R., & Dai, X. 2012, ApJ, 759, 20
Kochanek, C. S., 2013, ApJ in press [arXiv:1308.0013]
Kreidberg, L., Bailyn, C. D., Farr, W. M., & Kalogera, V. 2012, ApJ, 757, 36
Krüger, H., Landgraf, M., Altobelli, N., & Grün, E. 2007, Space Science Reviews, 130, 401
Kwok, S. 1975, ApJ, 198, 583
Landgraf, M., Baggaley, W. J., Grün, E., Krüger, H., & Linkert, G. 2000, Journal of Geophysical Research, 105, 10343
Laor, A., & Draine, B. T. 1993, ApJ, 402, 441
Lovegrove, E., & Woosley, S. E. 2013, ApJ, 769, 109
Meisel, D. D., Janches, D., & Mathews, J. D. 2002, ApJ, 579, 895
Murray, N., Weingartner, J. C., & Capobianco, C. 2004, ApJ, 600, 804
Nadezhin, D. K. 1980, Astrophysics and Space Science, 69, 115
Nanni, A., Bressan, A., Marigo, P., & Girardi, L. 2013, MNRAS, 434, 2390
O'Connor, E., & Ott, C. D. 2011, ApJ, 730, 70
Özel, F., Psaltis, D., Narayan, R., & McClintock, J. E. 2010, ApJ, 725, 1918
Pejcha, O., Thompson, T. A., & Kochanek, C. S. 2012, MNRAS, 424, 1570
Piro, A. L. 2013, ApJL, 768, L14
Slavin, J. D., Frisch, P. C., Müller, H.-R., et al. 2012, ApJ, 760, 46
Smartt, S. J., Eldridge, J. J., Crockett, R. M., & Maund, J. R. 2009, MNRAS, 395, 1409
Socrates, A., & Draine, B. T. 2009, ApJL, 702, L77
Szczygieł, D. M., Prieto, J. L., Kochanek, C. S., et al. 2012, ApJ, 750, 77
Thompson, T. A., Prieto, J. L., Stanek, K. Z., et al. 2009, ApJ, 705, 1364
Ugliano, M., Janka, H.-T., Marek, A., & Arcones, A. 2012, ApJ, 757, 69
Walmswell, J. J., & Eldridge, J. J. 2012, MNRAS, 419, 2054
Zhang, W., Woosley, S. E., & Heger, A. 2008, ApJ, 679, 639
Zinner, E. 1998, Annual Review of Earth and Planetary Sciences, 26, 147